Mucopolysaccharidosis type I (Hurler syndrome): oral and radiographic findings and ultrastructural/chemical features of enamel and dentin

Gunseli Guven, DDS, PhD,[a] Zafer C. Cehreli, DDS, PhD,[b] Ceyhan Altun, DDS, PhD,[a] Metin Şençimen, DDS, PhD,[c] Semra Ide, PhD,[d] Sevgi H. Bayari, PhD,[e] and Şeniz Karaçay, DDS, PhD,[f] Ankara, Turkey
GULHANE MEDICAL ACADEMY AND HACETTEPE UNIVERSITY

Mucopolysaccharidosis type I (Hurler syndrome, MPS I-H) is an autosomal recessive inborn error of metabolism due to deficient α-L-iduronidase enzyme activity and is characterized by accumulation of incompletely degraded glycosaminoglycans that generally lead to impairment of organ and body functions. This report presents oral, dental, and radiographic findings in a boy who presented with MPS I-H. Nine of the patient's primary teeth were extracted and investigated using scanning electron microscopy, x-ray diffraction analysis, and Fourier transform infrared spectroscopy. Compared with the teeth of otherwise healthy patients, MPS I-H–affected dentin was characterized by extremely narrow dentinal tubules, whose direction followed an irregular wave-like pattern. The enamel-dentin junction was defective, as evidenced by microgaps, and the enamel displayed irregular arrangement of prisms. The additional novel observation was made that the protein structure of enamel and dentin changed in MPS I-H–affected teeth. Also, an increase was observed in the relative mineral/matrix ratio of MPS I-H–affected dentin, indicating that its protein content had decreased in comparison with normal dentin. **(Oral Surg Oral Med Oral Pathol Oral Radiol Endod 2008;105:72-8)**

Mucopolysaccharidosis I (MPS I) is an autosomal recessive disorder caused by deficient or absent activity of the lysosomal hydrolase α-L-iduronidase.[1] This enzyme is responsible for the degradation of the glycosaminoglycans (GAGs) heparin sulfate and dermatan sulfate, and a deficiency in the enzyme leads to accumulation of these substances in various tissues.[2] The severe form of MPS I is also known as Hurler syndrome (MPS I-H) and is characterized by early onset of symptoms and central nervous system (CNS) effects.[3] Milder forms of MPS I are called attenuated, Hurler-Scheie, Scheie syndrome and have a late onset with no discernable effects on the CNS.[1]

[a]Assistant Professor, Department of Pediatric Dentistry, Center of Dental Sciences, Gulhane Medical Academy.
[b]Associate Professor, Department of Pediatric Dentistry, Faculty of Dentistry, Hacettepe University.
[c]Research Assistant, Department of Oral Surgery, Center of Dental Sciences, Gulhane Medical Academy.
[d]Professor, Department of Physics Engineering, Faculty of Engineering, Hacettepe University.
[e]Professor, Faculty of Education, Department of Physics, Hacettepe University.
[f]Assistant Professor, Department of Orthodontics, Center of Dental Sciences, Gulhane Medical Academy.
Received for publication Dec 12, 2006; returned for revision Jan 15, 2007; accepted for publication Feb 23, 2007.
1079-2104/$ - see front matter

doi:10.1016/j.tripleo.2007.02.015

The worldwide incidence of MPS I-H has been reported to be 1:100,000.[4] Death usually occurs before the second decade of life,[5] unless affected patients are treated by bone marrow transplantation.[1,2] In addition to dwarfism and mental retardation, patients with MPS I-H are characterized by skeletal malformations, hernias, cardiac disease and systemic hypertension, hepatosplenomegaly, and flexion conctractures.[6,7] The oral and dental findings of MPS I-H include hyperplastic gingiva, macroglossia, high-arched palate, short mandibular rami with abnormal condyles, spaced hypoplastic peg-shaped teeth with retarded eruption; and localized dentigerous cyst-like radiolucencies.[5,7-9]

Despite the well documented oral and dental features of MPS I-H, a search of the literature fails to demonstrate the ultrastructural and chemical properties of MPS I-H–affected teeth. The present report presents oral and radiographic findings in a boy with MPS I-H and demonstrates scanning electron microscopy (SEM), Fourier transform infrared spectroscopy (FTIR), and x-ray diffraction (XRD) findings in primary teeth extracted in accordance with the patient's treatment plan.

CASE REPORT

A 13-year-old boy was referred to the pediatric dentistry clinic for routine dental examination. The boy had been followed regularly by the hospital pediatrics unit for more than 10 years with the diagnosis of MPS I-H. Initial diagnosis

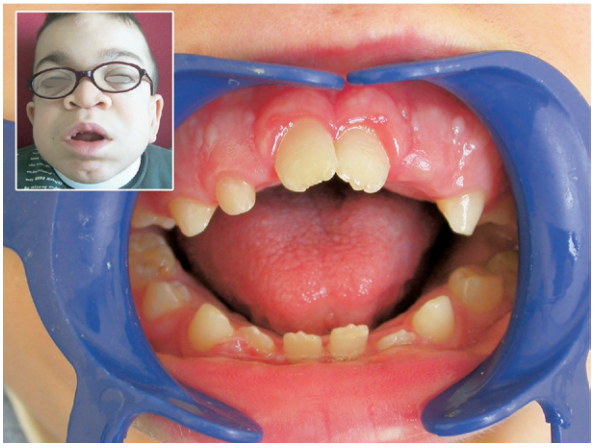

Fig. 1. Extraoral (*inset*) and intraoral view of the patient, demonstrating clinical features of mucopolysaccharidosis (MPS) type I.

of MPS was made at 10 months in light of clinical findings including coarse face, low nasal bridge, thoracolumbar gibbus, hepatosplenomegaly, inguinal hernia, and the following radiographic findings: spatulated ribs, gibbus deformity, vertebra bodies with beak-like projections on their lower anterior margins, and cuboidal changes of the metacarpals. A definitive diagnosis was made upon detection of a significant increase of dermatan sulphate in urine and a marked deficiency of α-L-iduronidase activity in his leukocytes. The boy was the first child of healthy nonconsanguineous parents whose second child was a 5-year-old healthy girl.

Clinically, the patient had retarded growth with a short stature for his chronologic age. Bony deformities, including kyphosis, rotated legs, and short stubby hands, were evident. In addition to bilateral corneal opacity, the following facial features were observed: oblique palpebral fissures, flat nasal bridge, flared nose, upturned nasal tip, and a large mouth with broad lips (Fig. 1). Despite an extremely limited opening of the patient's mouth, intraoral examination was easily made owing to the existing anterior open bite. The existing noncarious primary and permanent teeth were widely spaced and the gingival tissues were notably thick (Fig. 1). The enamel of primary teeth was slightly hypoplastic with a clinical appearance of pitted enamel, but the few erupted permanent teeth did not exhibit any enamel defect.

Panoramic radiograph taken at the same visit revealed cyst-like areas of bone destruction surrounding unerupted permanent teeth in the mandibular canine and ramus regions. The permanent second and third mandibular molars were located ectopically within both mandibular rami (Fig. 2). This was confirmed by a panoramic radiograph that was taken at the hospital at age 8 (Fig. 3). Presumably, the physicians did not note the developing cyst-like lesions around the mandibular permanent molars, which dramatically increased in size as evidenced by the last radiograph. In both radiographs, the pulp chamber of primary molars was notably small and pulp canals were extremely thin, giving an obliterated appearance. Additionally, both radiographs showed that the mandibular first molars were taurodont, and that the same entity was developing in the mandibular second molars, as evidenced by the final panoramic radiograph. Also the mandibular third molar had a microdont radiographic appearance. The hypoplastic appearance of the mandibular condyles confirmed the clinical finding of limited opening of the mandible. The treatment plan comprised extraction of maxillary first and second primary molars (bilaterally) and of the mandibular primary right canine, first and second molars, primary left canine, and second molar and marsupialization at both canine-premolar regions to allow eruption of the impacted teeth. The cystic lesions bilaterally surrounding the mandibular permanent first, second, and third molars were scheduled for another surgical intervention owing to the unfavorable osseous support of both mandibular rami.

The extracted teeth were investigated using SEM, XRD, and FTIR to characterize the samples and to determine the structural differences. To compare findings, the same type and number of teeth were collected from healthy patients undergoing orthodontic extractions in accordance with a study protocol approved by the Institutional Review Board. In both group of samples, half of the crowns were used for SEM evaluations and the other halves were processed for XRD and FTIR assays.

SEM EVALUATION

Ground sections were prepared from healthy and affected (patient's) teeth using a low-speed saw (Isomet 1000; Buehler, Lake Bluff, IL) under coolant water in the mesiodistal direction. The sections were dried by immersion in hexamethyldisilazane (Electron Microscopy Sciences, Hatfield, PA) for 30 minutes, placed on a filter paper inside a covered glass vial, and kept in vacuum for 24 hours. Subsequently, the specimens were sputter coated with gold-palladium (Balzers-SCd 050 sputter coater, Germany) for observation under the SEM (JSM-6400 V; JEOL, Tokyo, Japan) at 20 kV of accelerating voltage.

Results of the SEM observations showed that the diameters of dentinal tubules of MPS I–affected teeth were rather narrow at the pulpal end and that the dentinal tubules were smaller and more widely spaced than in normal dentin (Fig. 4, *A* and *B*). Also, the enamel-dentin junction was defective, as evidenced by microgaps (Fig. 4, *C* and *D*). Compared with normal dentin, the direction of tubules followed an irregular wavy pattern (Fig. 5, *A* and *B*). The MPS I–affected enamel displayed irregular arrangement of prisms in an occasionally globular pattern (Figs. 5, *C* and *D*).

XRD ANALYSIS

The 20 values of x-ray powder diffraction patterns of normal and affected samples were measured with CuK_{α} radiation ($\lambda = 1.54184$ Å) on a Philips manual spectrogoniometer (LabX, Midland, Canada) over the range

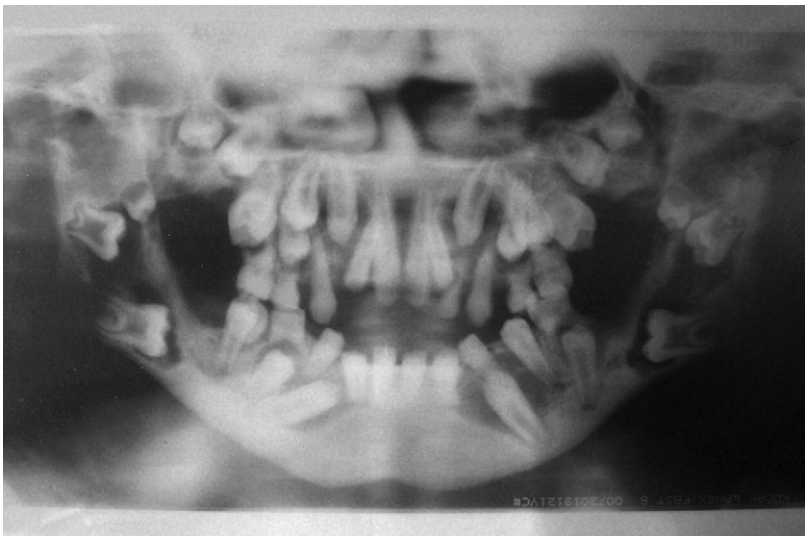

Fig. 2. Panoramic radiograph taken at the first visit (age 13), showing extensive cystic lesions and erupting impacted permanent teeth. Note hypoplastic mandibular condyles and taurodont permanent mandibular molars.

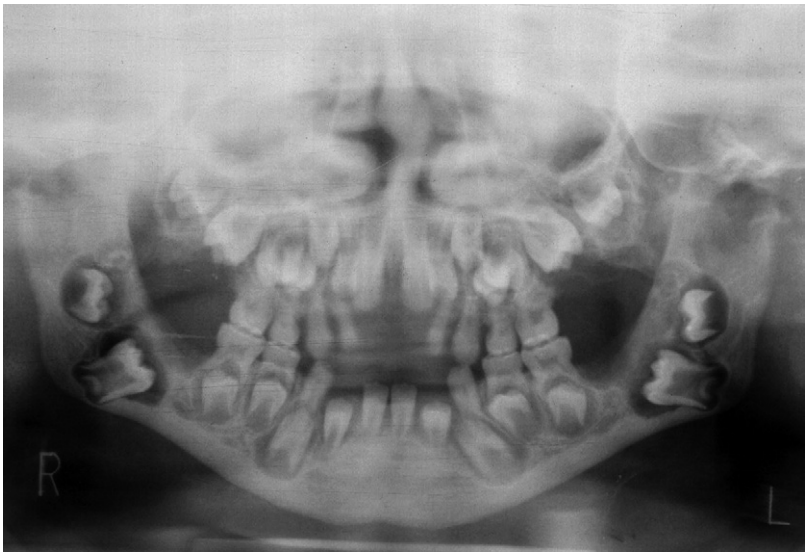

Fig. 3. Panoramic radiograph of the patient taken at age 8. Note development of taurodontism in the permanent mandibular molars. The pulp space of primary molars are notably small.

$5° \leq 20 \leq 50°$ (where 0 is half the angle of deviation of the diffracted rays from the incident x-rays).

The hydroxyapatite (HA) crystallite size of each sample was calculated using Scherrer's equation and Bragg reflections (at 002) and was found to be approximately 17.7 nm, which corresponds to the normal peak of HA. Thus, all diffraction patterns of the studied samples indicated the known characteristic peaks of HA, and there were not any notable differences in the crystal structure of HA in the samples (Fig. 6).

FTIR ANALYSIS

Powdered samples were examined as KBr pellets (1 mg sample per 100 mg KBr). The FTIR spectra were recorded at room temperature in the range 400-4000 cm^{-1} on a Perkin Elmer Spectrum One FTIR spectrometer (Boston, MA). Interferograms were averaged for 400 scans at 4-cm^{-1} resolution. Background spectra were collected under identical conditions with the samples and automatically subtracted from spectra of samples. The ν_1, ν_3 phosphate (PO_4^{3-}) stretching

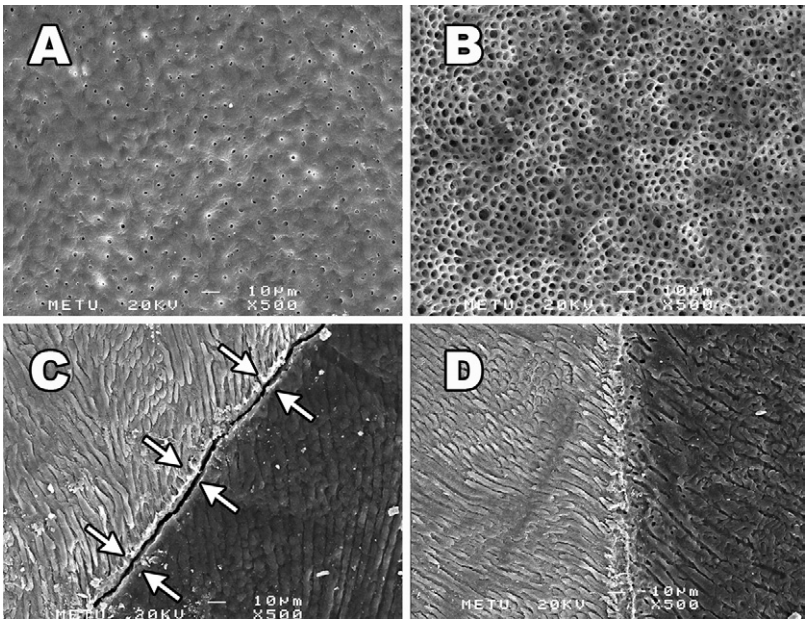

Fig. 4. **A,** Scanning electron micrograph of MPS I–affected dentin depicting dentinal tubules as viewed from the pulp chamber. **B,** View of dentin tubules (normal dentin) from the same aspect. **C,** Enamel-dentin junction of MPS I–affected tooth. Note gap formation between two tissues. **D,** Enamel-dentin junction of normal tooth.

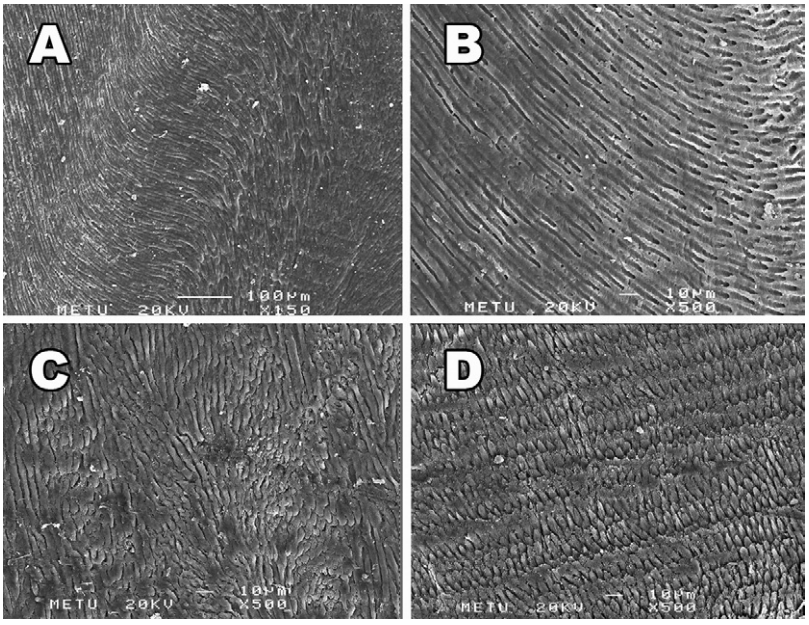

Fig. 5. **A,** Wave-like appearance of dentinal tubules in MPS I–affected tooth. **B,** View of dentin tubules in normal dentin. **C,** MPS type I–affected enamel. **D,** Normal enamel.

(900-1200 cm^{-1}), the amide I (1595-1720 cm^{-1}), and the ν_2 carbonate (CO_3^{2-}) (850-890 cm^{-1}) bands were baseline corrected.[10,11] Then, mineral-matrix ratio was obtained by taking the ratio of the integrated area under the peaks at ν_1, ν_3 (PO_4^{3-}) (900-1200 cm^{-1}) stretching and amide I (1580-1725 cm^{-1}) regions. The relative carbonate content was calculated from FTIR spectra by taking the ratio of the integrated area of the ν_2 CO_3^{2-}

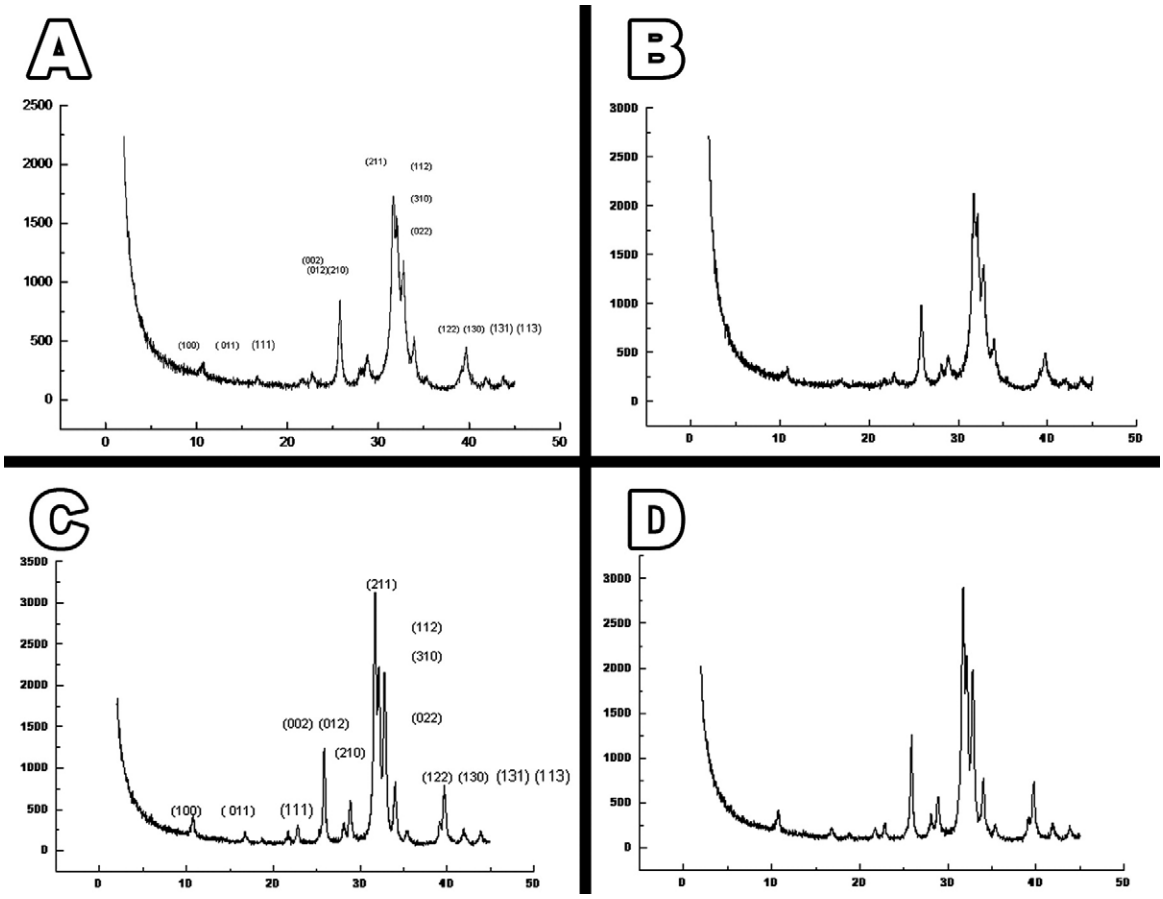

Fig. 6. **A** and **B,** X-ray powder patterns of normal and MPS I–affected dentin, respectively. **C** and **D,** X-ray powder patterns of normal and MPS I–affected enamel, respectively.

(850-890 cm^{-1}) band and of the ν_1, ν_3 (PO_4^{3-}) stretching band.[10-15]

As seen in Fig. 7, the frequency of the amide I bands displayed a shift to higher values in MPH I-H–affected dentin (1659 cm^{-1} and 1663 cm^{-1} for normal and affected dentin, respectively) and MPH I-H–affected enamel (1646 cm^{-1} and 1654 cm^{-1} for normal and affected enamel, respectively), as a result of alterations in the protein structure of both hard tissues. Additionally, the relative mineral-matrix ratio increased in MPS I-H–affected dentin. The mineral-matrix ratio is indicative of the relative quantity of mineral present in calcified tissues, and an increase in the amount of phosphate indicates that its protein content had decreased compared with normal dentin.

DISCUSSION

In general, the clinical and radiographic features of the patient presented here are in line with those of earlier reports. However, except for the radiographic view of the unerupted maxillary permanent first molars, there was no evidence of peg-shaped teeth. The radiographic observations that were considered novel in the present case are decreased pulp space in primary molars, taurodontism, and ectopy of mandibular molars. Also of importance is the radiographic demonstration of hypoplastic condyles[16] being contributory to the clinical finding of limited opening of the patient's mouth. Other features seen in MPS I-H but not observed in the present case were calcification of the stylohyoid ligament and flattening of the anterior region of the hard palate. The latter finding is thought to be classic for Hurler syndrome[2,9] and occurs owing to the pressure of the tongue which exhibits macroglossia because of deposition of GAGs within its structure.[9]

Dentigerous cyst-like lesions that result in progressive destruction of the bone are common in MPS I-H and are generally identified bilaterally in the mandible.[9] As confirmed by the panoramic radiograph taken at age 8, the lesions appeared to start within the dental follicle of mandibular first molars, and was probably left unnoticed by the physician. If the patient was referred to

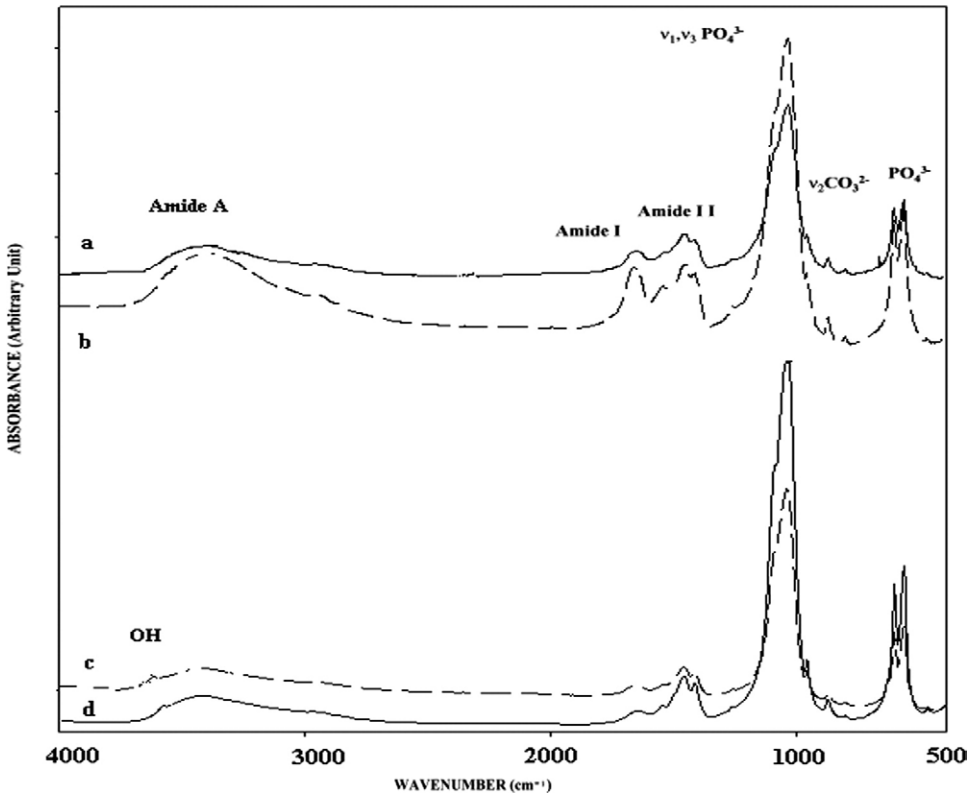

Fig. 7. Fourier transform infrared spectra of: normal dentin (a, *solid line*), MPS I–affected dentin (b, *dashed line*); MPS I–affected enamel (c, *dashed line*); and normal enamel (d, *solid line*). The amide I mode in normal dentin appears at 1659 cm^{-1} and in affected dentin at 1663 cm^{-1}. This mode appears in normal enamel at 1646 cm^{-1} and in MPH I-H–affected enamel at 1654 cm^{-1}.

the dentist, an earlier surgical intervention could have been possible, because dimensions of the radiolucency around the molar crowns exceeded the normally accepted limit of 3 mm for a dental follicle.[2] It is also noteworthy to mention that the onset of the cyst-like lesions in both canine-premolar regions was not evident radiographically at age 8. In the present case, marsupialization was the preferred method of treating the cysts in the canine-premolar regions (along with primary tooth extractions), because the technique can maintain the impacted tooth in its cavity and promote its eruption.[17-19] For the lesions of bilateral mandibular rami, a surgical intervention was planned later, because the extent of osseous support was greatly compromised.

The SEM findings obtained from the extracted primary teeth of the patient suggest that the accumulation of GAGs in MPS I-H may also exhibit consequences in the enamel and dentin tissues. In addition to the irregular arrangement of enamel prisms which might contribute to the clinical finding of slightly hypoplastic enamel, the microgaps between enamel and dentin and the narrow diameter of dentinal tubules at the pulpal end were not considered coincidental. What was observed as tubule narrowing at the submicron level is probably indicative of the macroscopically evident excessive hard tissue deposition in dentin, which may logically manifest as decreased pulp space, a finding that was observed in primary molars on both panoramic radiographs.

Although XRD analysis did not show any difference between the crystal structures of HA in normal and MPS I-H–affected teeth, results of the FTIR analysis provided evidence for changes in the protein structure of MPS I-H–affected enamel and dentin, as evidenced by the higher frequency shift in the amide I band, the most intense band in protein IR spectra which is sensitive to the protein conformation.[20] Additionally, an increase was observed in the relative mineral-matrix ratio of MPS I-H–affected dentin. The mineral-matrix ratio is indicative of the relative quantity of mineral present in calcified tissues, and an increase in the amount of phosphate indicates that the amount of protein had decreased relatively.[15,21]

Whether the present ultramorphologic and chemical findings are typical to MPS I-H, and whether they have any clinical impact, can only be verified by investiga-

tion of MPS I–affected primary and permanent teeth in future cases. However, we believe that these findings are relevant and can contribute to an understanding of the pathomechanism responsible for the development of peculiar changes in enamel and dentin. Also of interest is whether bone marrow transplantation or enzyme replacement therapy would have impact on such dental changes associated with MPS I-H.

REFERENCES

1. Bjoraker KJ, Delaney K, Peters C, Krivit W, Shapiro EG. Long-term outcomes of adaptive functions for children with mucopolysaccharidosis I (Hurler syndrome) treated with hematopoietic stem cell transplantation. J Dev Behav Pediatr 2006;27:290-6.
2. Hingston EJ, Hunter ML, Hunter B, Drage N. Hurler's syndrome: dental findings in a case treated with bone marrow transplantation in infancy. Int J Paediatr Dent 2006;16:207-12.
3. Whitley CB. The mucopolysaccharidoses. In: Beighton P, editor. McKusick's heritable diseases of connective tissue. 5th ed. St Louis (MO): Mosby; 1993. p. 367-499.
4. Wraith JE. The first 5 years of clinical experience with laronidase enzyme replacement therapy for mucopolysaccharidosis I. Expert Opin Pharmacother 2005;6:489-506.
5. Keith O, Scully C, Weidmann GM. Orofacial features of Scheie (Hurler-Scheie) syndrome (alpha-L-iduronidase deficiency). Oral Surg Oral Med Oral Pathol Oral Radiol Endod 1990; 70:70-4.
6. Hinek A, Wilson SE. Impaired elastogenesis in Hurler disease: dermatan sulfate accumulation linked to deficiency in elastin-binding protein and elastic fiber assembly. Am J Pathol 2000;156:925-38.
7. Thomas S, Tandon S. Hurler syndrome: a case report. J Clin Pediatr Dent 2000;24:335-8.
8. Worth HM. Hurler's syndrome. A study of radiologic appearances in the jaws. Oral Surg Oral Med Oral Pathol Oral Radiol Endod 1966;22:21-35.
9. Gardner DG. The oral manifestations of Hurler's syndrome. Oral Surg Oral Med Oral Pathol Oral Radiol Endod 1971;32:46-57.
10. Camacho NP, Landis WJ, Boskey AL. Mineral changes in a mouse model of osteogenesis imperfecta detected by Fourier transform infrared microscopy. Connect Tissue Res 1996; 35:259-65.
11. Camacho NP, Rinnerthaler S, Paschalis EP, Mendelsohn R, Boskey AL, Fratzl P. Complementary information on bone ultrastructure from scanning small angle x-ray scattering and Fourier-transform infrared microspectroscopy. Bone 1999; 25:287-93.
12. Bohic S, Rey C, Legrand A, Sfihi H, Rohanizadeh R, Martel C, et al. Characterization of the trabecular rat bone mineral: effect of ovariectomy and bisphosphonate treatment. Bone 2000;26: 341-8.
13. Gadaleta SJ, Paschalis EP, Betts F, Mendelsohn R, Boskey AL. Fourier transform infrared spectroscopy of the solution-mediated conversion of amorphous calcium phosphate to hydroxyapatite: new correlations between X-ray diffraction and infrared data. Calcif Tissue Int 1996;58:9-16.
14. Pleshko N, Boskey A, Mendelsohn R. Novel infrared spectroscopic method for the determination of crystallinity of hydroxyapatite minerals. Biophys J 1991;60:786-93.
15. Boyar H, Zorlu F, Mut M, Severcan F. The effects of chronic hypoperfusion on rat cranial bone mineral and organic matrix. A Fourier transform infrared spectroscopy study. Anal Bioanal Chem 2004;379:433-8.
16. MacLeod SP, Macintyre DR. Bilateral hypoplasia of mandibular condyles in Hurler's syndrome. Oral Surg Oral Med Oral Pathol Oral Radiol Endod 1993;75:659-60.
17. Takagi S, Koyama S. Guided eruption of an impacted second premolar associated with a dentigerous cyst in the maxillary sinus of a 6-year-old child. J Oral Maxillofac Surg 1998; 56:237-9.
18. Moro Antonio JM, Puente M. Surgical-orthodontic treatment of an impacted canine with a dentigerous cyst. J Clin Orthod 2001;35:491-3.
19. Ertas U, Yavuz MS. Interesting eruption of 4 teeth associated with a large dentigerous cyst in mandible by only marsupialization. J Oral Maxillofac Surg 2003;61:728-30.
20. Karande P, Jain A, Ergun K, Kispersky V, Mitragotri S. Design principles of chemical penetration enhancers for transdermal drug delivery. Proc Natl Acad Sci U S A 2005;102:4688-93.
21. Verdelis K, Crenshaw MA, Paschalis EP, Doty S, Atti E, Boskey AL. Spectroscopic imaging of mineral maturation in bovine dentin. J Dent Res 2003;82:697-702.

Reprint requests:

Dr. Günseli Güven
Gülhane Askeri Tıp Akademisi
Dişhekimliği Bilimleri Merkezi
Pedodonti Anabilim Dalı
Etlik
Ankara
Turkey
gunseliguven@yahoo.com